

**Cell Reports, Volume 30**

**Supplemental Information**

**NONU-1 Encodes a Conserved Endonuclease**

**Required for mRNA Translation Surveillance**

**Marissa L. Glover, A. Max. Burroughs, Parissa C. Monem, Thea A. Egelhofer, Makena N. Pule, L. Aravind, and Joshua A. Arribere**

## SUPPLEMENTAL FIGURES

### **Figure S1: Two strains show linkage to an area of chromosome III lacking known Nonstop mRNA Decay factors (related to Figure 1 and STAR Methods)**

Genetic maps for three strains showing linkage (and lack thereof) to chromosomes II, III, and IV. WJA0648 contains a mutation in *skih-2* on chromosome IV. WJA0675 and WJA0641 contain mutations in *f26a1.13/14* (renamed *nonu-1*) on chromosome III. X-axis shows position along the chromosome in megabases (Mb). See STAR Methods for a description of the Hawaiian mapping procedure and variant calling. This technique narrows down the causative mutation to a large swath of one chromosome, after which we manually inspected the region of interest to identify possible mutations (subsequently verified by CRISPR/Cas9).

### **Figure S2: *f26a1.13/14* encode a single functional gene (related to Figure 1 and STAR Methods)**

A. Gene diagrams for *f26a1.13* and *f26a1.14*. Prior annotations indicated on top, with rectangles and lines representing exons and introns, respectively. New annotation below, along with the location of each of three premature stop codon mutations (*srf* alleles) that exhibit identical phenotypes in a Nonstop mRNA reporter strain. Data in parts (B-D) are vertically aligned with annotations in part (A).

B. Public ESTs that span the proposed previously unannotated splice junction.

C. Published RNA-seq data from (Hendriks et al., 2014) showing reads spanning the proposed previously unannotated splice junction. Inset (C') zooms in on the region of interest, with reads supporting the junction highlighted (blue). Antisense reads in red.

D. Published Ribo-seq data from (Hendriks et al., 2014) showing ribosome footprints spanning the proposed previously unannotated splice junction. Inset (D') zooms in on the region of

interest, with reads supporting the junction highlighted (blue). Note there is a similar density of Ribo-seq reads throughout the entire gene body of both *f26a1.13* and *f26a1.14*, consistent with the idea they represent a single translational unit.

**Figure S3: Conservation and evolution of the Smr domain in the IF3-C fold framework (related to Figure 2 and STAR Methods)**

- A. Extended multiple sequence alignment of representatives of domains from the TusA-Alba-Smr assemblage. Secondary structure shown on top, and consensus on which alignment is colored provided on bottom line.
- B. Phylogenetic tree of evolutionary relationships between different IF3-C fold domains, with key evolutionary transitions labeled to the left of the diagram. Tree branches are colored according to occurrence of the domain in the respective kingdom (Archaea, Bacteria, and/or Eukarya). Some evolutionary relationships are uncertain (dotted lines). Structural renderings of boxed domains (TusA, Smr, RNaseG/E) are shown in Figure 2B. Functional annotations for lineages in red boxes below names are as follows: 'RB', RNA-binding; 'RP', RNA-processing. Here, top-down view of RNaseG/E is provided to emphasize the importance of dimerization in the metal-binding nuclease active site.
- C. Broader phylogeny depicted as stylized tree of all known Smr domain families. Nodes supported by bootstrap >75% are marked by brown circles. Dotted lines in tree indicate uncertainty in phylogenetic placement. Representative domain architectures observed within each family provided to the right of monophyletic, collapsed tree branches. Individual domains found within a single polypeptide are represented by distinct shapes labeled by name. Dotted lines around a domain indicate absence in some organisms of the listed phylogenetic distribution for each architecture, provided below architectural depiction. Red circle represents

the N-terminal basic stretch described in the text. Red box represents a variable-length charged region characteristic of members of the ypl199c-like clade.

**Figure S4: Multiplicative and non-multiplicative effects of *skih-2* and *nonu-1* on phenotypes (related to Figure 3 and STAR Methods)**

A. RNA-seq read counts in the indicated strains. RNA-seq was performed (see STAR Methods), and read counts for all mRNAs is shown (black dots) with *unc-54* highlighted (green dot). Off-diagonal genes indicate increased mRNA expression in one strain relative to the other. Note axes are log-scaled.

B. Brood sizes for the indicated strains. Each X represents the number of progeny from a single animal from that strain. 12 animals were examined per strain. P-values from Student's T-test.

C. Y-axis shows log<sub>2</sub> fold change for gene expression changes between the indicated mutant strains and wild type for all genes with at least 30 reads in wild type (different read cutoffs in wild type yielded similar results). *nonu-1* (red) and *skih-2* (blue) targets are defined as mRNAs that are upregulated in the respective mutant strains relative to wild type (as determined by DESeq, see STAR Methods). P-value from Mann Whitney U test comparing the indicated subset of genes to all genes. Note that unlike *unc-54*, targets of *nonu-1* and *skih-2* fail to exhibit a further increase in mRNA expression in the double mutant. Many genes' mRNAs that increased in either *skih-2* (13 of 27) or *nonu-1* (20 of 31) were derived from genes known to be developmentally regulated (Hendriks et al., 2014), consistent with a mild developmental delay between wild type and mutant strains. Furthermore, as a class, mRNAs whose levels increased in either *skih-2* or *nonu-1* did not exhibit any further increase in the double mutant (Figure S4C), in contrast to the behavior of the *unc-54(Nonstop)* reporter. A biological replicate of these data produced similar results.

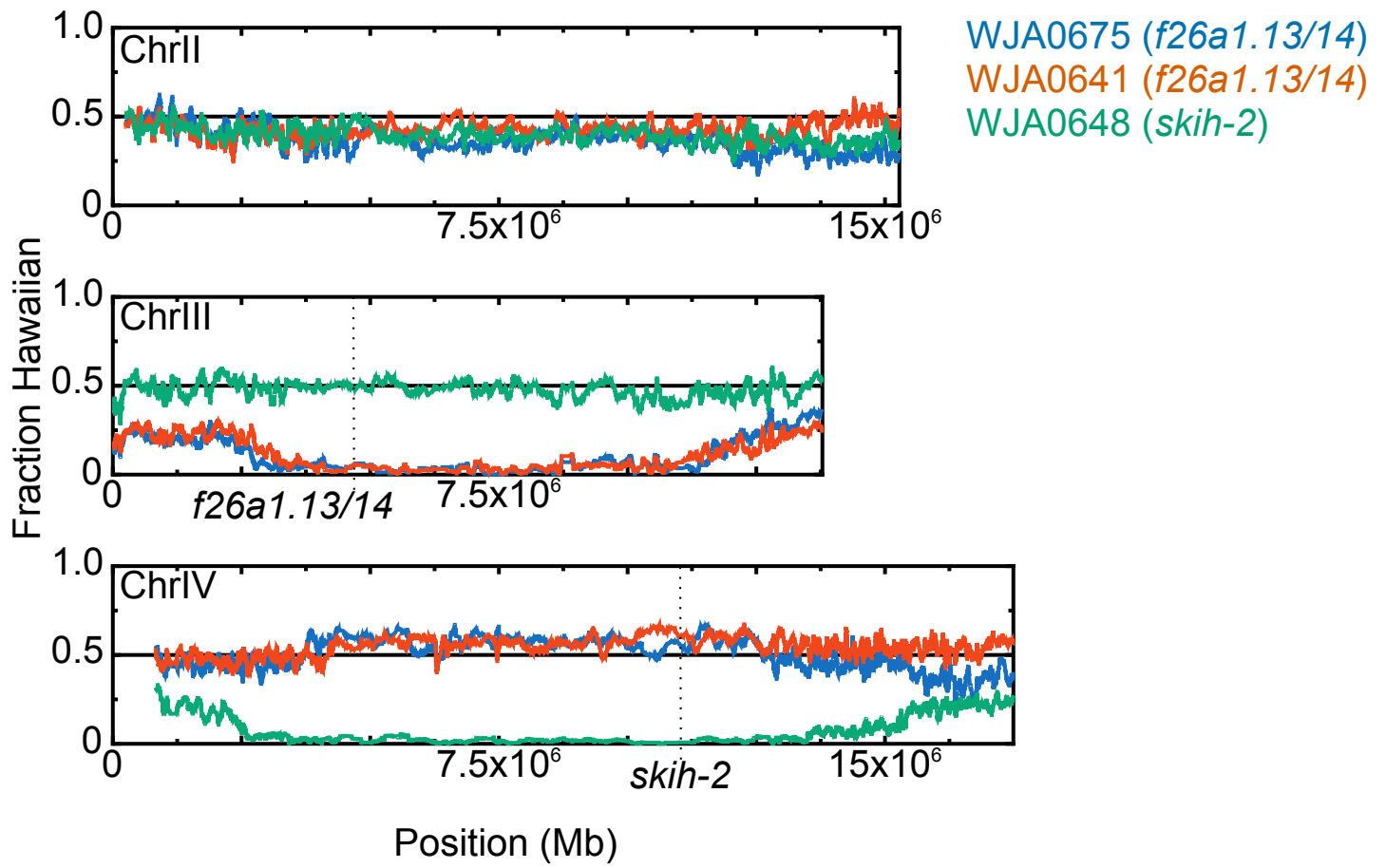


Figure S1: Two strains show linkage to an area of chromosome III lacking known Nonstop mRNA Decay factors (related to Figure 1 and STAR Methods)

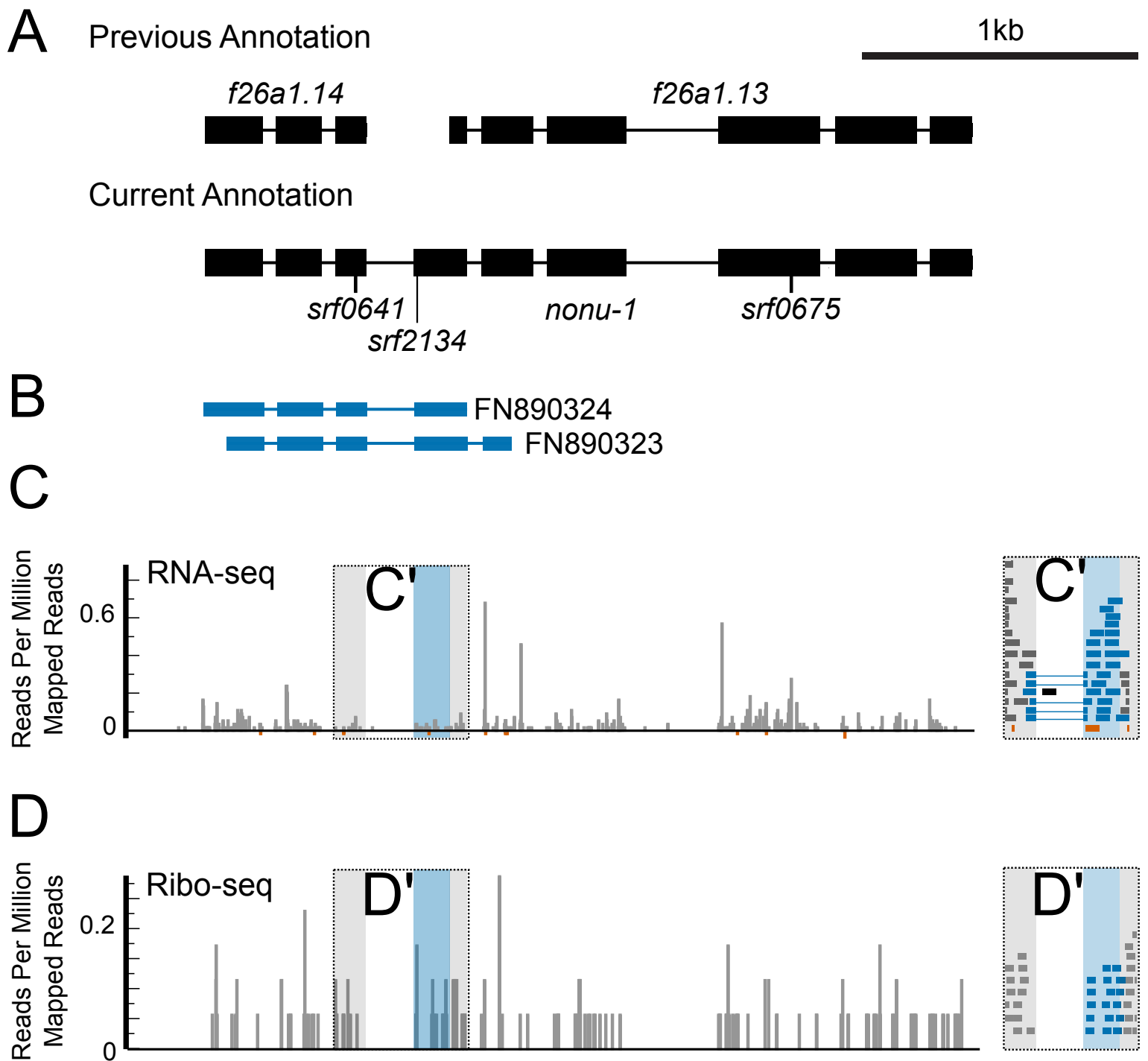


Figure S2: *f26a1.13/14* encode a single functional gene (related to Figure 1 and STAR Methods)

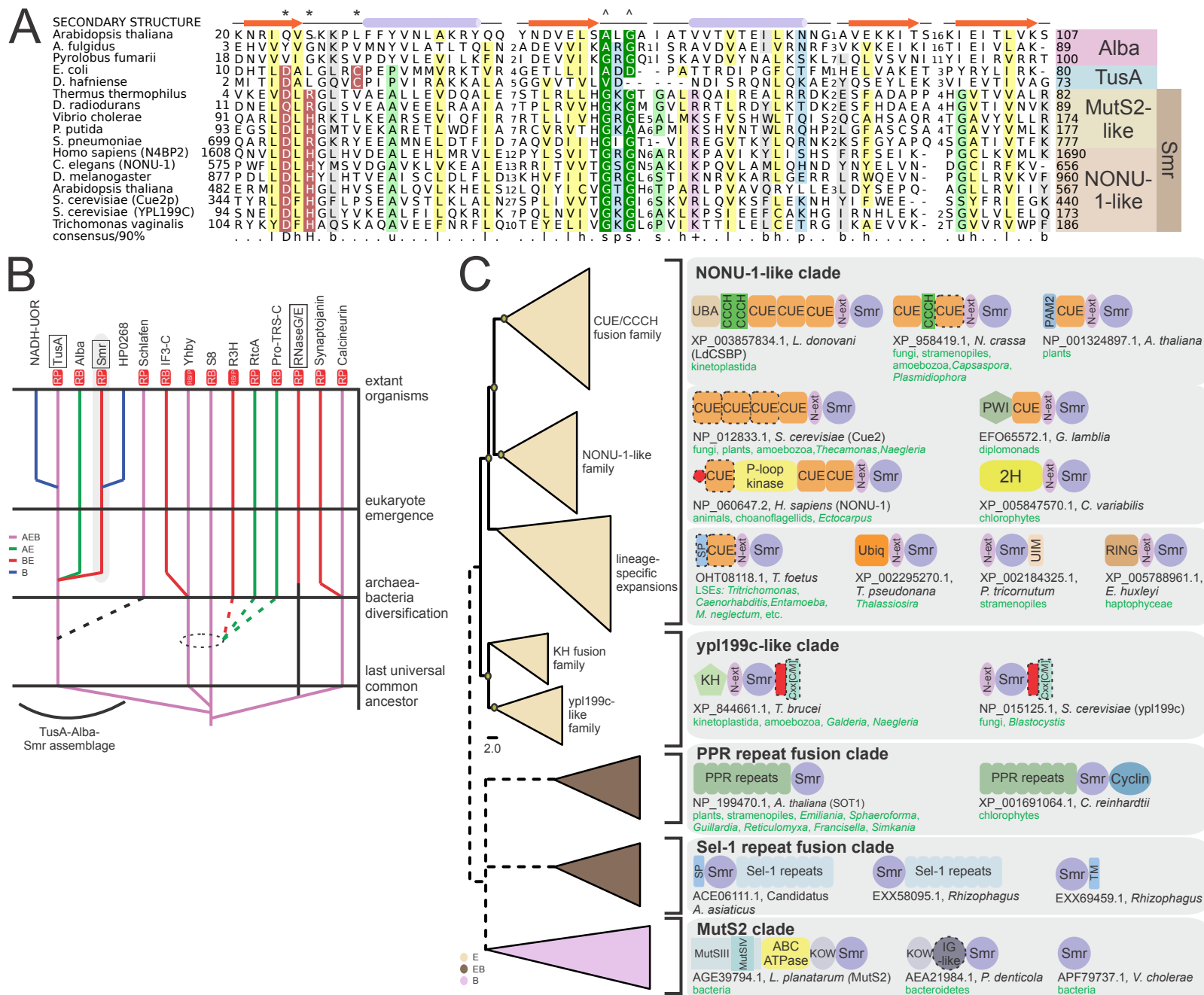


Figure S3: Conservation and evolution of the Smr domain in the IF3-C fold framework (related to Figure 2 and STAR Methods)

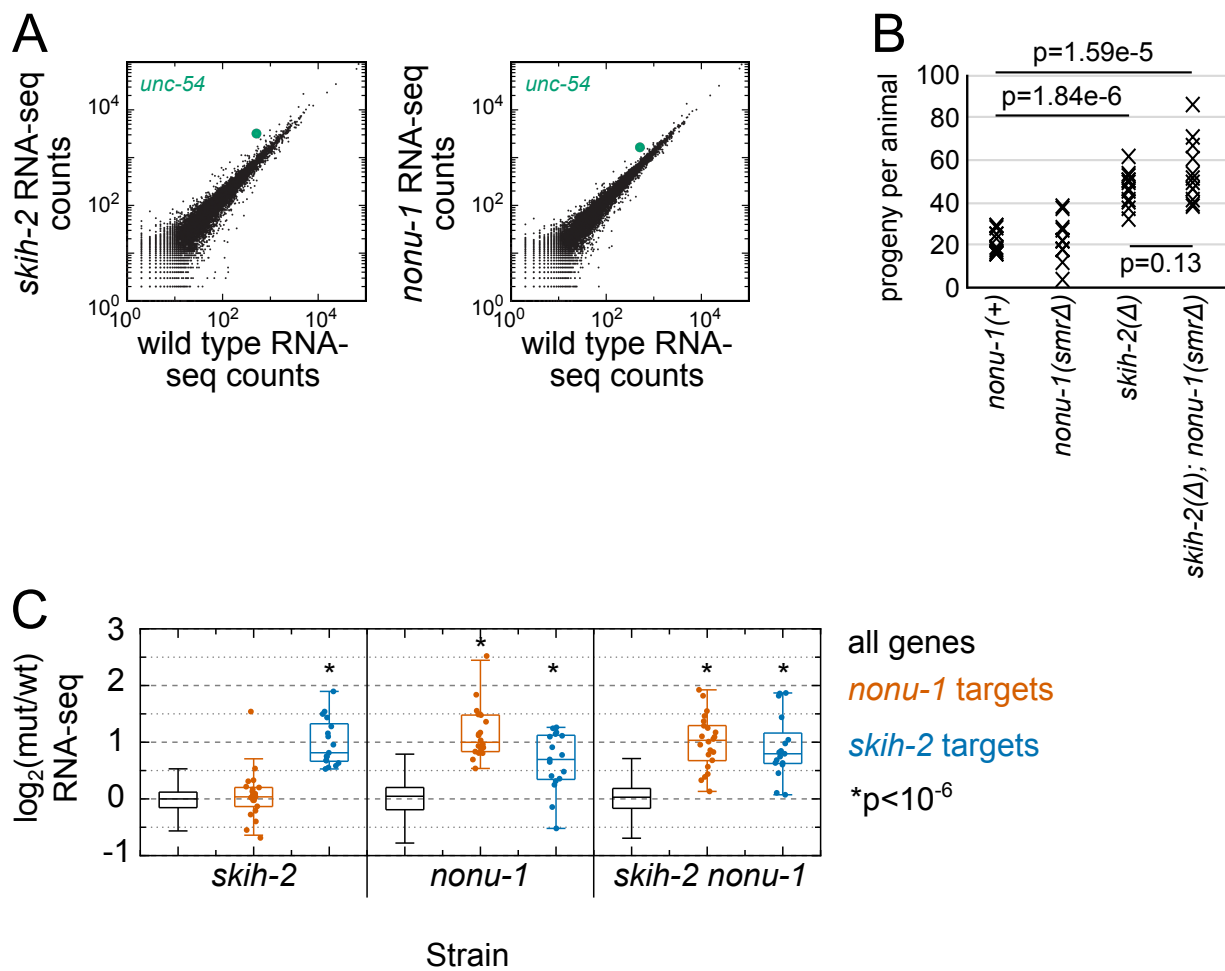


Figure S4: Multiplicative and non-multiplicative effects of *skih-2* and *nonu-1* on phenotypes (related to Figure 3 and STAR Methods)